Flomeko 2000 - IMEKO TC9 Conference
Salvador, Bahia, BRAZIL
4-8 June, 2000

MODELLING OF TRANSIT TIME ULTRASONIC FLOWMETERS IN THEORETICAL ASYMMETRIC FLOW

†*Pamela I. Moore, †Gregor J. Brown, *Brian P. Stimpson

†National Engineering Laboratory, Scottish Enterprise Park, East Kilbride, Scotland, G75 0QU

*Department of Electronic and Electrical Engineering, University of Strathclyde Royal College Building, 204 George Street, Glasgow,Scotland,G1 1XW

Abstract: Velocity profile is the definition given to the distribution of velocity in the axial direction over the cross-section of the pipe. This distribution is not usually flat and can vary dramatically depending on the properties of the fluid and the configuration of the pipe in which it flows. Fully developed flow is well defined for most values of Reynolds number however distorted flow is not. Ultrasonic flowmeters are affected by such distortions in the flow profile often resulting in erroneous measurements. For this reason correction to or prediction of distorted profiles has sparked great interest in the design and application of ultrasonic flowmeters. Multi-path ultrasonic flowmeters are widely used in industry and many utilise a bounce-path technique. This document describes an analysis of the effect of theoretical asymmetric flow profiles on four transit time ultrasonic configurations utilising no more than two paths.

Key words: ultrasonic flow measurement, transit time, asymmetric flow, installation effects, computational fluid dynamics

1 INTRODUCTION

Velocity profile is the definition given to the distribution of velocity in the axial direction over the cross-section of the pipe. This distribution is not usually flat and can vary dramatically depending on the properties of the flow and the pipe configurations upstream. Fully developed flow is well defined for most values of Reynolds number but distorted flow is not. Ultrasonic flowmeters are affected by such distortions in the flow profile often resulting in erroneous measurements. For this reason correction to or prediction of distorted profiles have sparked great interest in ultrasonic flowmeter manufacturers.

This document describes an analysis of the effect of two sets of theoretical asymmetric flow profiles on four different meter configurations. The first set used was produced by Salami [1] to investigate flow rate estimation based on point velocity integration methods in the 1970's. Salami's work includes 23 profiles, five of which are used here. The second set was produced using data obtained from a computational fluid dynamics (CFD) simulation of a double out of plane bend.

The two sets of profiles are similar and part of the investigation assesses the usefulness of the Salami profiles compared to those produced using CFD generated data. Also contained in the paper is a comparison of four ultrasonic meter configurations that employ no more than two paths. These include two configurations that utilise more than one traverse of the pipe per path and two that do not. Multiple traverses are achieved by implementing reflections from the inside wall of the pipe.

2 THEORETICAL PROFILES

The theoretical profiles of Salami [1] are based on the power law in smooth pipes (1), superimposed with some function of radial and angular distance, r and θ respectively. It is the superimposed function that creates the asymmetric flow. All profiles adhere to zero flow at the pipe wall as would be expected in practice, and there is a portion, close to the wall that can be described by the power law.

$$\frac{V}{V_c} = \left(1 - \frac{r}{R}\right)^{\frac{1}{n}} \quad (1)$$

V is the true point velocity, V_c the velocity along the central axis of the pipe, R the radius of the pipe, r the distance from the centre of the pipe and *n* is a coefficient dependent on *Re*. For the purposes of this document V_c and R both have the value of 1. The functions described by Salami are of three mathematical types of which one is used here, (2).

$$V = (1 - r)^{\frac{1}{n}} + mr(1 - r)^{\frac{1}{k}} f(\theta) \quad (2)$$

Here f(θ) is a defined function of θ where *n, k, m* are constants within each profile. The profiles described here were chosen because they resemble the asymmetric flow that results downstream of two out of plane bends. Five profiles were chosen and the contour plots are shown in figure 1.

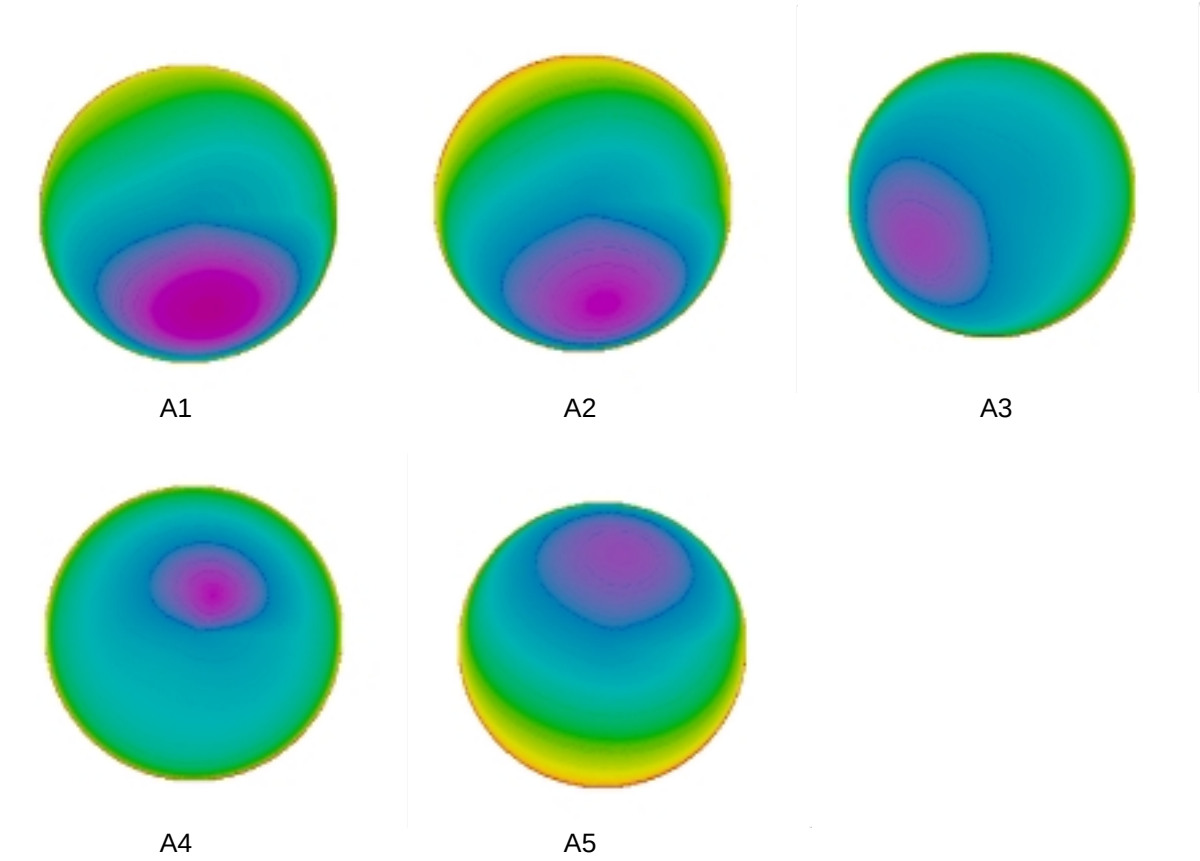

Figure 1. Contour plots of theoretical profiles

The order in which the profiles appear in [1] has been changed in this document. Table 2 shows both the profile name as referred to here and that used by Salami (in brackets). The table also lists the parameters used in the mathematical functions that describe the profiles.

Calculation of the true mean cross-sectional velocity, $\bar{v}$, can be obtained from a particular theoretical mathematical function by integration and this is used as a reference against which the measured flow velocity is compared. A disadvantage of the profiles listed in table 2 is the presence of a discontinuity at θ = 0, 2π radians in profiles A1, A2, A4 and A5. This can be found by taking the derivative of (2) with respect to θ.

Because these profiles are artificial there is some question of the validity of them. However, there is some evidence in the literature to indicate that the profiles are useful. Salami suggests, in reference [2], that some of his profiles resemble measured profiles from the open literature and this is supported by Franc [3]. In [1] Salami states that profiles A3 and A5 are similar to those downstream of bends and indeed Walus [4] suggests that (2) may be used generally to describe asymmetric flow in pipes. Further, an example of an extensive study which includes the analysis of fourteen of the profiles described in [1] is reference [5] .

Table 2 Values of parameters

Profile Id.	*n*	*m*	*k*	f(θ)	F(θ)= $\int_0^{2\pi} f(\theta)d\theta$
A1 (P6)	9	$-\frac{0.5}{\pi}$	4	$\theta \sin\theta$	-2π
A2 (P17)	7	$-\frac{0.4}{\pi}$	9	$\theta \sin\theta$	-2π
A3 (P8)	9	$\frac{0.04}{\pi}$	4	$(\theta^2\text{-}1)(1\text{-}\cos\theta)^2$	$4\pi^3 - \frac{21\pi}{2}$
A4 (P1)	9	3.3170	0.5	$e^{-a\theta}\sin\theta$, a=0.5	$\frac{(1-e^{-2\pi a})}{(a^2+1)} \Rightarrow \frac{(1-e^{-\pi})}{1.25}$
A5 (P12)	7	0.6846	9	$e^{-a\theta}\sin\theta$, a=0.2	$\frac{(1-e^{-2\pi a})}{(a^2+1)} \Rightarrow \frac{(1-e^{-\pi})}{1.04}$

The advantages of using theoretical profiles are clear where they resemble experimental flows. Computational time is small as is the requirement for highly powered processing compared to the use of CFD simulations. Also, the velocity at any point is known without the need for interpolation of cell values as is the case in CFD simulations. Further advantage can be obtained when the true flow rate can be computed exactly, where the function is integrable over the cross sectional area of the pipe.

3 COMPUTATIONAL FLUID DYNAMICS PROFILES

The CFD profiles were taken from a simulation of a double out of plane bend. The software used was Fluent 5.3. This is a multi-purpose, commercial code that is widely used for a range of industrial applications. Figure 2 shows the computational mesh used. The radius of curvature was one diameter in both bends. The simulation was performed in two stages. The first was the simulation of the flow through the bend where the inlet boundary condition was defined as being fully developed flow. Figure 2 shows that the mesh is extended beyond the outlet of the bend so that the outlet boundary condition did not influence the flow through the fixture itself. The profile at the outlet of the second bend was used as the inlet condition for the second part of the simulation, the test section, the mesh of which is shown in figure 3.

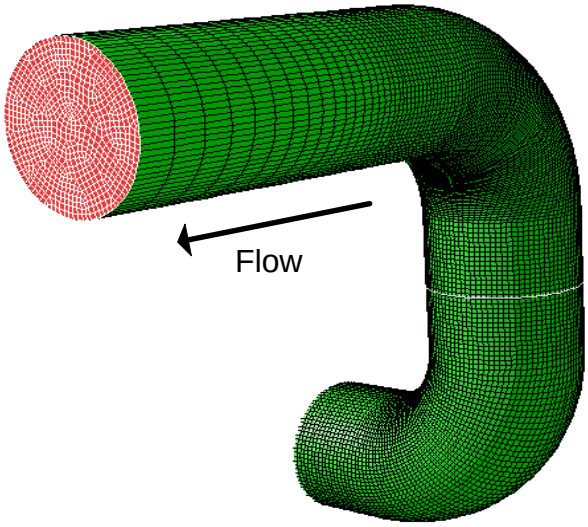

Figure 2. Computational mesh of double out of plane bend

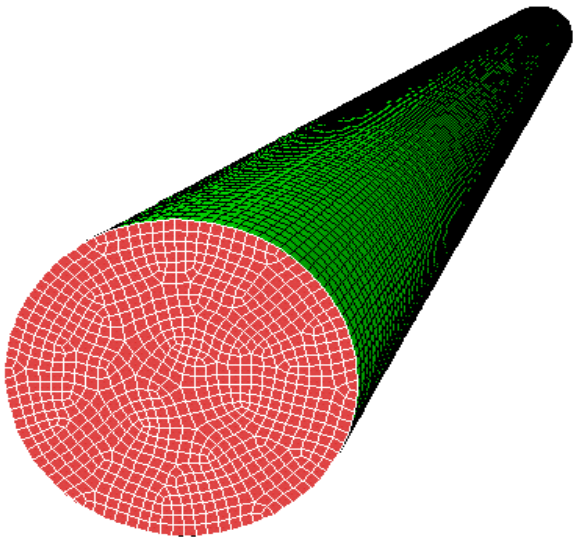

Figure 3. Computational mesh of the test section of length 30 D

The fluid was chosen to be water at standard pressure and temperature, therefore the density was set at 1000 kgm^{-3} and the viscosity was set to be 0.001 $kgm^{-1}s^{-1}$. The flow rate was ~ 157 ls^{-1}, and the diameter of the pipe was 0.203 m. A number of turbulence models were available in the Fluent code, the most popular for general CFD work being the standard k-ε model [6], the Renormalisation group k-ε (RNG) [7] model and the Reynolds stress model (RSM)[8, 9]. A comparison of these three models showed that the RSM model most reliably reproduced experimental results therefore this model was utilised.

Five profiles were produced by using data from the CFD simulation. Cross sectional data was extracted at 1, 2, 3, 4 and 5 meters from the inlet of the test section. For each set of data a polynomial was fitted to represent the profile. This was done because the data output from a CFD simulation is

restricted to cell centre and node values, the position of which are dependent on the mesh used, whereas the use of the polynomial allowed the velocity at any point to be known in the cross section. The resulting contour plots of the profiles are shown in figure 4.

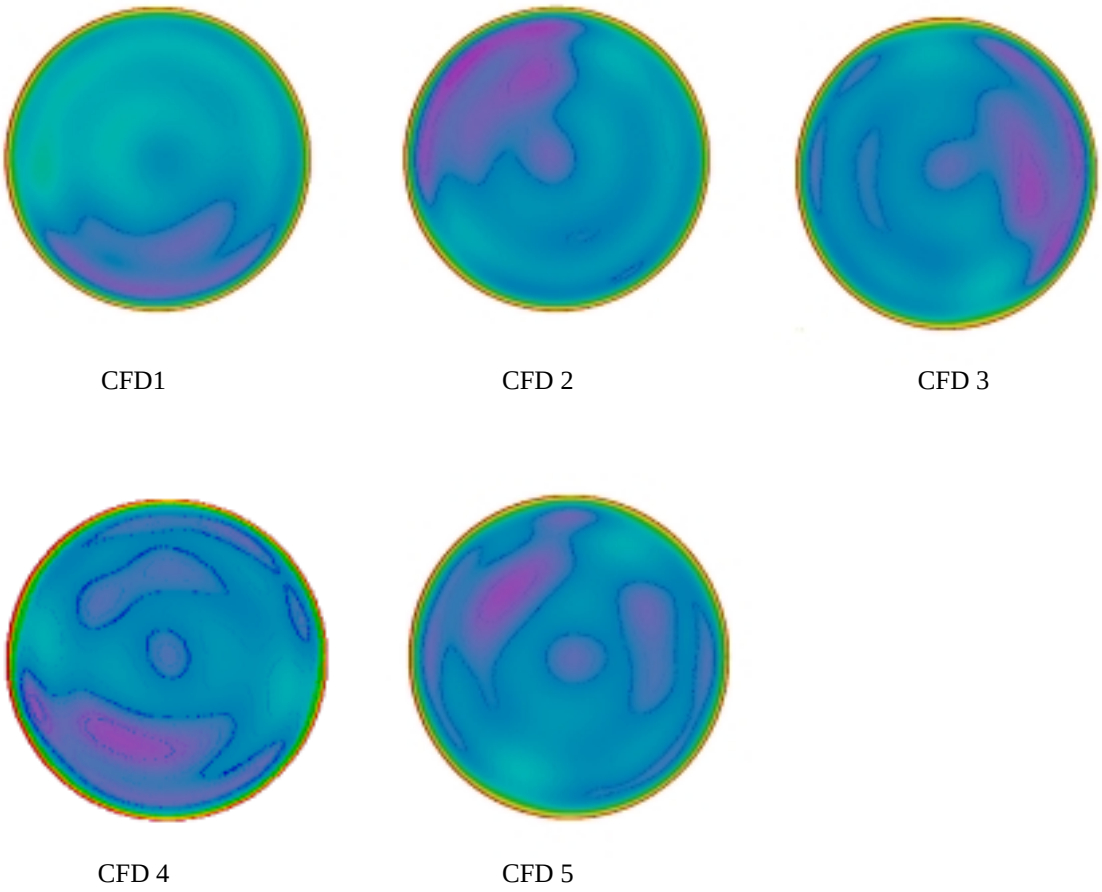

Figure 4. Contour plots of CFD data fitted with polynomials

4 ESTIMATION OF MEAN FLOW VELOCITY

Ultrasonic flowmeters measure flow velocity via the transmission of sound waves through the fluid. There are various techniques that may be employed but this paper discusses the transit time measurement technique. The transit time method of measurement is the most commonly used in ultrasonic flow metering. The measurement is made by transmitting a pulse from a transducer through the fluid to a second transducer positioned downstream in the pipe and back again.

The transit time principle operates by measuring the difference in the time taken for the signal to travel up and downstream. The component of flow velocity adds to or subtracts from the apparent velocity of sound in the fluid in the downstream and upstream measurements respectively. Appropriate flow media are gases or liquids but the fluid must be single phase for the meter to perform well. A simple diagram of such a flowmeter is shown in figure 5.

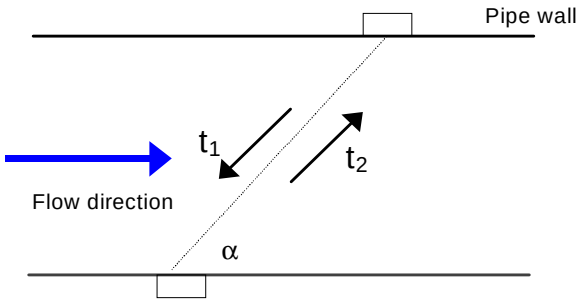

Figure 5. Simple diagram of ultrasonic flowmeter

The propagation velocity of the sound pulse is the vector sum of the velocity of sound and the flow velocity in the direction of propagation. Therefore the transit time of the upstream, t_1, and downstream, t_2, signals can be expressed as (3) and (4) respectively:

$$t_1 = \int_0^t \frac{dl}{c - V_z(l)\cos\alpha} \tag{3}$$

$$t_2 = \int_0^t \frac{dl}{c + V_z(l)\cos\alpha} \tag{4}$$

Where *l* is the path length, c the velocity of sound in the fluid, $V_z(l)$ is the axial flow velocity measured at point d*l* along the path and α is the angle of inclination. It can be shown that (5) is found by substituting (3) in to (4).

$$V_{z\,mean} = \frac{l\,\Delta t}{2\,t_1 t_2 \cos\alpha} \tag{5}$$

This is the basic principle of the transit time flowmeter used in the measurement of 3-dimensional flow. Many designs have been published which build on this, some more useful than others. Several times in the literature transit time flowmeters have been reviewed. Examples of these can be found in the form of references [10-14].

5 CONFIGURATIONS

The configurations tested, which utilise no more than two paths, are shown in figure 6. The first two configurations are commonly used with respect to clamp on meters as they utilise paths along the diameter. The second two configurations are interesting because, although they appear to use six paths in the first and five in the second, they can actually be implemented using only two and one paths respectively. This is achieved by bouncing the pulse of ultrasound off the pipe wall until it reaches the angular position it was sent from. Broekgaarden [15] introduced configurations involving bounce paths with multiple reflections as did Lynnworth [16]. Utilising configurations with bounce-paths means that there are less transducers required and, from Lynnworths point of view, this type of configuration is advantageous when there is limited access to the pipe.

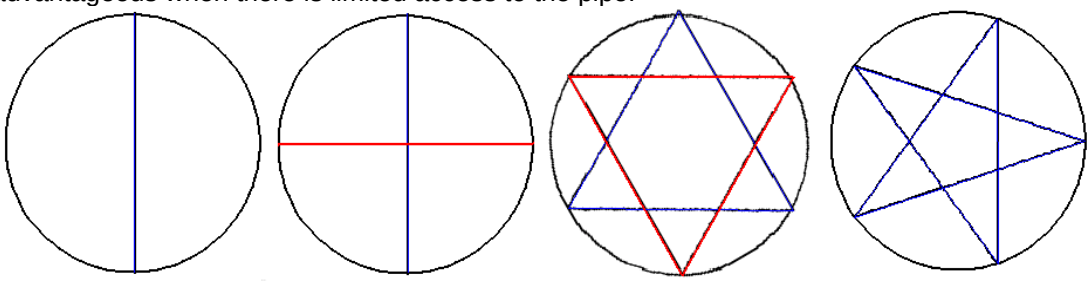

Figure 6. Ultrasonic flowmeter configurations

Measurement of $V_{z\,mean}$ in the theoretical profiles is done by integration of the point velocities along the path in the theoretical profiles using (6):

$$V_{z\,mean} = \frac{\iint_{\text{path i}} f(r,\theta)}{l} \tag{6}$$

Calculation of the true mean velocity is done similarly by integrating over the whole cross-section of the pipe (7):

$$\bar{v} = \iint f(r,\theta) \tag{7}$$

The meters discussed here measure the flow rate by taking the average of the path velocities using (8):

$$V = \frac{\sum_{i=1}^{n} (V_{z\,mean})_i}{n} \tag{8}$$

where $(V_{z\,mean})_i$ is the velocity calculated using (6) along path i and n is the number of paths utilised in the configuration.

6 COMPARING DEVIATIONS IN THE HYDRODYNAMIC FACTOR WITH RESPECT TO ORIENTATION

The hydrodynamic factor, H, is a dimensionless parameter that is defined as the ratio of the true mean velocity in the pipe to that which is measured, (9):

$$H = \frac{\bar{v}}{V} \tag{9}$$

That is to say, a hydrodynamic factor of 1 is achieved if the measurement equates exactly with the true mean velocity. The hydrodynamic factor is used as a parameter to compare the effect of the profiles on the four configurations. The second parameter used in the comparison is a measure of the range of H determined by the configuration for a given profile. This is called the orientation sensitivity factor and is defined as S:

$$S = H_{\max} - H_{\min} \tag{10}$$

H was calculated in each profile for a period of π radians at increments of π/90. Figures 1 and 4 show the contour plots of these profiles. However, although the profiles are similar they are oriented differently from each other. Therefore, in order to compare them they were shifted such that they were approximately oriented similar to profiles A1 and A2. For example, profile A3 was rotated ~ π/3 radians anticlockwise and profile CFD3 was rotated ~ π/2 radians clockwise. Figures 7 - 10 show the results of the hydrodynamic factor plotted against the angle of orientation for each configuration.

All four graphs show that measurement in profiles A1-A5 show a similar trend to that in profiles CFD1-CFD5, however, there are some differences. Figure 7 and 8 indicate that H measured in CFD1 - CFD5 is ~ 0.06 larger than that measured in profiles A1 - A5. Figures 9 and 10 show that the difference is ~ 0.02 and 0.04 respectively. It appears that the difference between the two types of profiles decreases with an increase in the number of traverses utilised in the meter configuration.

Although H is plotted across the range $0 < \theta < \pi$ radians the orthogonal, double triangle and five pointed star configurations have a period of less than this. Therefore, the data is repeated once the period of rotation has been reached. This is shown in figures 8 - 10 by a dotted line. No dotted line is shown on figure 7 since the period of the diametrical configuration is π radians.

From figures 7 and 8 it is noticed that there is a discontinuity at 0, 2π radians and also at π/2 in figure 8. These are caused by the discontinuity of the function in equation (2) where θ=0, 2π. However, it is clear that the general trend is similar to profiles CFD1 - CFD5. There is no discontinuity shown by the other two configurations, double triangle and five point star because they do not consist of any measurement paths along the diameter. However, that is not to say that the discontinuity does not affect the measurement of these configurations, it is simply less obvious.

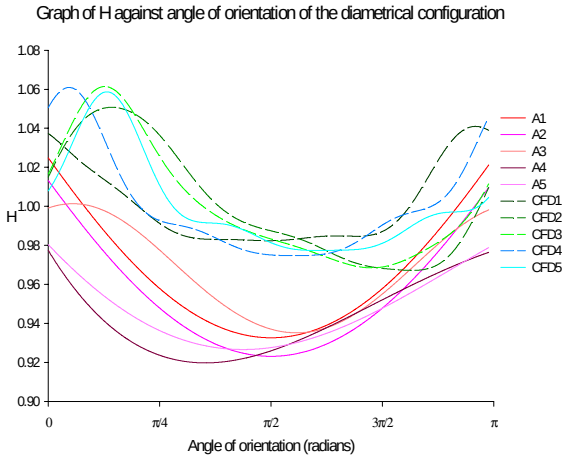

Figure 7. Graph of H against angle of orientation of the diametrical configuration

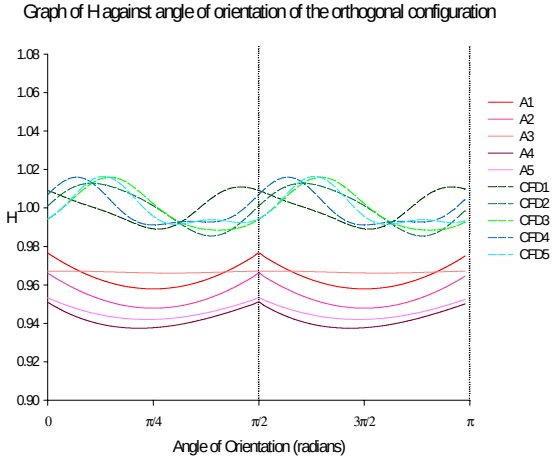

Figure 8. Graph of H against angle of orientation of the orthogonal configuration

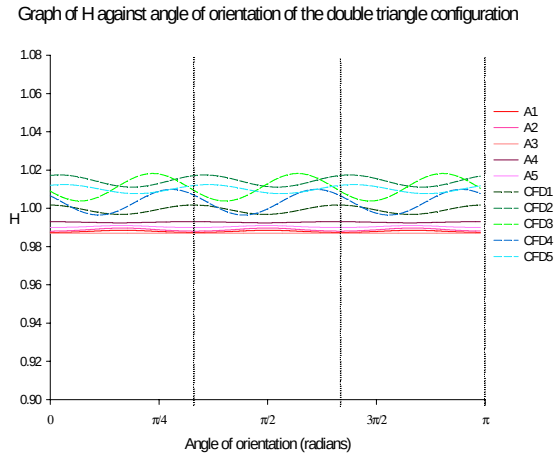

Figure 9. Graph of H against angle of orientation of the double triangle configuration

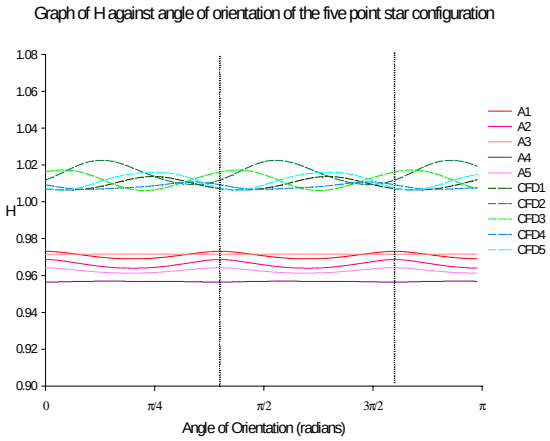

Figure 10. Graph of H against angle of orientation of the five point star configuration

The orientation sensitivity factor, S, is a measure of the range of H measured when the configuration is presented with a profile at various orientations. Therefore the measurement of S indicates the sensitivity of the configuration to orientation within the profile. Figures 11 - 14 show the graphs of S against profile for each of the four configurations. These graphs indicate the comparison of ranges of H measured in each profile.

Figure 11 shows that the range measured by the diametrical configuration is very similar in both types of profiles. A similar trend is found in figure 12 which shows S measured with the orthogonal configuration, however, this time S is less than approximately 1/3 that measured by the diametrical configuration. This is a large decrease and indicates that the additional path of the orthogonal configuration plays a significant role in the reduction of the sensitivity to orientation.

Continuing the comparison, figure 13 shows a further reduction in S as measured by the double triangle configuration and figure 14 indicates that the five pointed star configuration measures similar values. It is clear that as the number of traverses in the pipe is increased the value of S measured decreases, thus the sensitivity of the configuration to orientation decreases.

Figure 15 shows a comparison of the measurement of S in each of the profile types. The chart shows the of the average orientation sensitivity factor measured by each configuration in each profile type.

It can be seen that the average orientation sensitivity factor of the diametrical configuration is > 0.05. Introducing a second diametrical path to produce the orthogonal configuration decreases the average orientation sensitivity factor to < 0.03. However, by far the most effective configurations in terms of sensitivity to orientation are the double triangle and the five point star configurations.

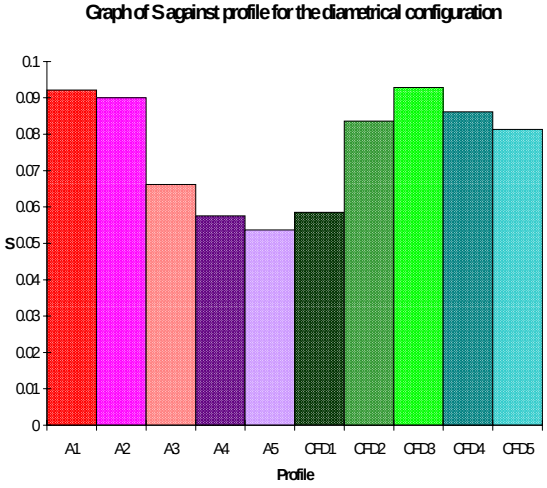

Figure 11. Graph of S against profile for the diametrical configuration

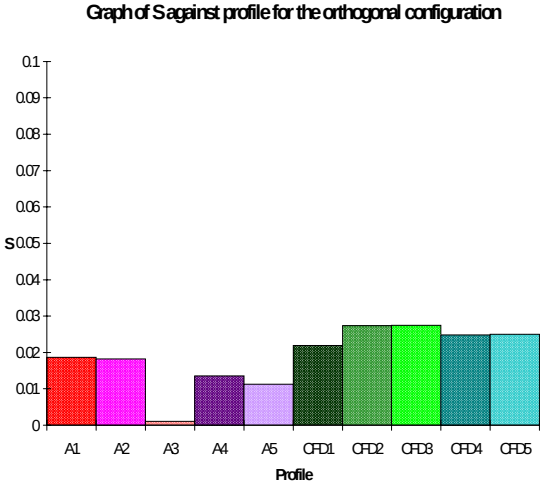

Figure 12. Graph of S against profile for the orthogonal configuration

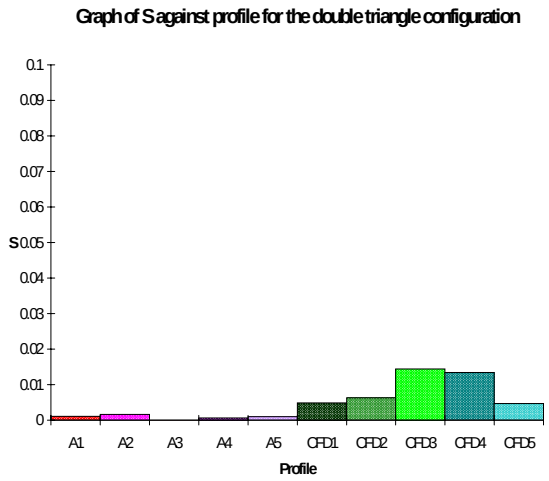

Figure 13. Graph of S against profile for the double triangle configuration

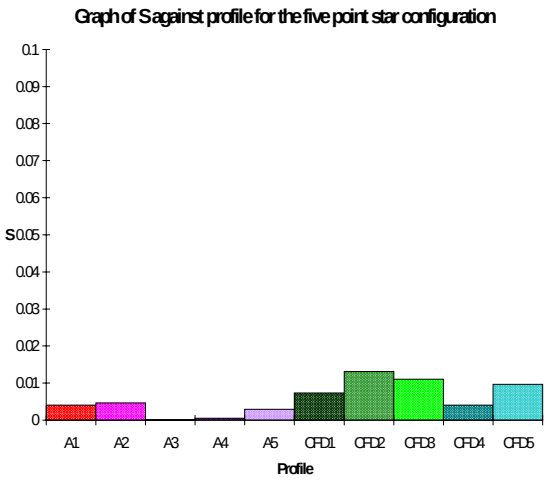

Figure 14. Graph of S against profile for five point star configuration

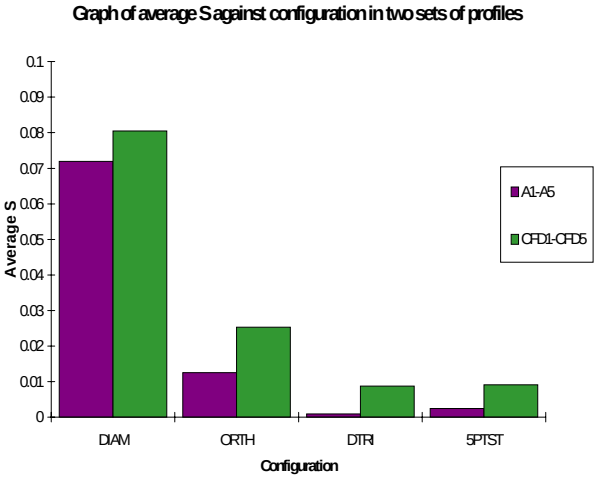

Figure 15. Graph of average S against configuration in profiles A1 - A5 and CFD1 - CFD5.

7 CONCLUSION

The document has discussed the effect of two types of theoretical flow profiles on four ultrasonic meter configurations. The comparison of the two profile types suggests that the mathematically defined profiles of the type described by (2) can be used to indicate the general trend of measurements made downstream of a double out of plane bend.

However, there are some disadvantages to be considered. These profiles have a discontinuity present at $\theta = 0, 2\pi$ which affects any measurement made in that region of the pipe. They also indicate systematic shifts in both H and S. However, these minor problems may be improved by firstly considering the use of a function which is continuous at $\theta = 0, 2\pi$. Secondly, the CFD profiles used in this document were based on flow at one flow rate and with one fluid. It may be that the profiles A1 - A5 show a greater resemblance to profiles produced either with a different fluid, flow rate or a different pipe bend radius of curvature.

There are effectively some configurations less sensitive to the effects of orientation with respect to asymmetric flow than others. It has been shown that the use of bounce paths is highly effective for the purposes described here. Increasing the number of traverses of the ultrasonic pulse within the pipe decreases the sensitivity of the configuration to orientation within the profile. The use of bounce paths is recommended since as little as two transducers can be implemented to produce a meter of small sensitivity.

ACKNOWLEDGMENTS

Pamela Moore is an Associate of the Postgraduate Training Partnership (PTP) between the National Engineering Laboratory (NEL) and the University of Strathclyde. The PTP scheme is a joint initiative of the UK's Department of Trade and Industry (DTI) and the Engineering Sciences Research

Council (EPSRC). The PTP scheme is supported by a grant from the DTI. Pamela Moore gratefully acknowledges grant support from both the EPSRC and NEL.

REFERENCES

[1] L. A. Salami, Application of a Computer to Asymmetric Flow Measurement in Circular Pipes, *Trans. Inst. M C*, 1984. **6**(4): p. 197-206.
[2] L. A. Salami, Errors in the Velocity-Area Method of Measuring Asymmetric Flows in Circular Pipes, . 1971, University of Southampton: Southampton
[3] S. Franc, C. Heilmann and H. E. Siekmann, Point-velocity methods for flow-rate measurements in asymmetric pipe flow, *Flow. Meas. Instrum.*, 1996. **7**(3/4): p. 201-209.
[4] S. Walus, The use of the ultrasonic flowmeter in the conditions other than normal, *FLOMEKO*, University of Melbourne, Australia, Aug 20-23, 1985, p. 171-176
[5] P. I. Moore, G. J. Brown and B. P. Stimpson, Ultrasonic measurement of asymmetric flow, *FEDSM2000*, Boston, Massachusetts, June 11-15th, 2000, p.
[6] B. E. Launder and D. B. Spalding, The numerical computation of turbulent flows, *Computer methods in applied mechanics and engineering*, 1974. **3**: p. 269-289.
[7] V. Yakhot and S. A. Orszag, Renormalization Group Analysis of Turbulence. I. Basic Theory, *Journal of Scientific Computing*, 1986. **1**(1): p. 3-50.
[8] B. E. Launder, Second-moment closure: present... and future?, *Int. J. Heat and Fluid Flow*, 1989. **10**(4): p. 282-300.
[9] B. E. Launder, G. J. Reece and W. Rodi, Progress in the development of a Reynolds - stress turbulence closure, *J. Fluid Mech.*, 1975. **68**(3): p. 537-566.
[10] R. C. Asher, *Ultrasonic Sensors*, . Institute of Physics, 1997.
[11] A. E. Brown, *Ultrasonic flowmeters*, . Flow measurement Practical guides for measurement and control, ed. D. W. Spitzer. Instrument Society of America, 1991.
[12] K. I. Jesperson, A review of the use of ultrasonics in flow measurement, . 1973, National Engineering Laboratory: Glasgow
[13] L. C. Lynnworth, *Ultrasonic Measurements for Process Control*, . Academic Press, 1989.
[14] L. C. Lynnworth, *Ultrasonic flowmeters*, . Physical Acoustics. Vol. XIV, 1979.
[15] G. J. Broekgaarden and H. Lammerse, Ultrasonic gas flow measurements in reflection mode in underground pipelines, *Intl. Symp. fluid flow*, United Kingdom, Nov, 1986, p.
[16] L. C. Lynnworth, T. H. Nguyen and J. A. True, Flowmeter designs: small ID; small OD; limited length; limited access, *Ultrasonics Symp.*, 1986, p. 587-593

Corresponding Author: Ms P I Moore, National Engineering Laboratory, Scottish Enterprise Park, East Kilbride, Scotland, G75 0QU, phone +44 (0) 1355 272927. E-mail: pmoore@nel.uk